The conformational, electronic and spectral properties of chalcones: A density functional theory study

ARTICLE *in* JOURNAL OF MOLECULAR STRUCTURE THEOCHEM · MAY 2009

Impact Factor: 1.37 · DOI: 10.1016/j.theochem.2009.01.034

2 AUTHORS, INCLUDING:

Yunsheng Xue
Xuzhou Medical College
20 PUBLICATIONS **121** CITATIONS

SEE PROFILE

Journal of Molecular Structure: THEOCHEM 901 (2009) 226–231

Contents lists available at ScienceDirect

Journal of Molecular Structure: THEOCHEM

journal homepage: www.elsevier.com/locate/theochem

The conformational, electronic and spectral properties of chalcones: A density functional theory study

Yunsheng Xue [a,*], Xuedong Gong [b]

[a] School of Pharmacy, Xuzhou Medical College, No. 209, Tongshan Road, Xuzhou, Jiangsu 221004, China
[b] Department of Chemistry, Nanjing University of Science and Technology, Nanjing 210094, China

ARTICLE INFO

Article history:
Received 13 September 2008
Received in revised form 29 January 2009
Accepted 29 January 2009
Available online 8 February 2009

Keywords:
Chalcones
Electronic absorption spectrum
Substitution effect
TD-DFT/PCM

ABSTRACT

The ground-state geometries and electronic spectra of *trans*-chalcone and its derivatives have been studied with the density functional theory (DFT) and time-dependent density functional theory (TD-DFT). A wide panel of theoretical methods has been used, with various basis sets and DFT functionals, to assess a level of theory that would lead to converged excitation energies. Solvent effects on the excitation energies were computed through the integral equation formalism of the polarizable continuum model (IEFPCM). It turns out that PCM-TD-PBE1PBE/6-31G//PBE1PBE /6-31G(d) approach provides reliable λ_{max}. The calculated absorption spectral properties are in good agreement with the experimental results. The results suggest the assignments for the lowest five electronic transitions observed experimentally for *trans*-(*s-cis*)-chalcone in solution. Calculated substitution shifts for *trans*-(*s-cis*)-chalcone derivatives are in qualitatively agreement with experimental data.

1. Introduction

Chalcones form a group of open-chain flavonoids, in which two aromatic rings are linked by a three-carbon α,β-unsaturated carbonyl system (see Scheme 1). Numerous biological activities have been observed for these compounds over the past 20 years, including anti-ulcer, anti-cancer, anti-mitotic, anti-inflammatory, anti-malarial, anti-fungal, anti-HIV and anti-oxidant activities [1–8]. Beyond these very important applications in biological chemistry, chalcones have interesting optical properties including high extinction coefficients for absorption in the UV, and significant nonlinear optical responses [9,10].

Therefore, it is clear that understanding the nature of the main electronic transitions responsible for the absorption spectrum of chalcones is a problem of some practical interest. Despite of many investigations existed, the available experimental picture for chalcone cannot be considered complete. Some bands are quite strongly overlapped and another isomer, *trans*-(*s-trans*)-chalcone, may coexists in solution with *trans*-(*s-cis*)-chalcone. These make the interpretation of the UV spectrum of *trans*-chalcone complicate, and therefore some disputable opinions exist.

Nowadays, the quantum-chemical tools offer a competitive alternative for the interpretation of experimental data arising from industrial interest and applications. There have been some calculations on the electronic spectrum of chalcone using semiempirical and *ab initio* HF methods [11–15]. The semiempirical calculations, PPP [11,12] and ZNDO/S3-CI [13], seem to be essentially in disagreement. On the other hand, using *ab initio* CIS/HF, Oumi et al. [15] studied chalcones, but the differences reported between gas-phase theoretical and solvated experimental λ_{max} are quite large (0.7 eV on average); Moreover, their discussion was restrict to the three low-lying electronic transitions observed experimentally. Therefore, theoretical description of the electronic transitions in chalcone is not completely clear. On the other hand, TD-DFT is often found to be robust and efficient for evaluating the low-lying excited spectrum of conjugated molecules and has been the subject of countless applications. In addition, bulk solvent effects can be accounted for when using TD-DFT. However, to our knowledge, only two papers have reported on the use of DFT for the study of chalcones, showing that the electron affinities and anti-oxidant properties of different substituted chalcones can be successfully reproduced, respectively [16,17]. These works did not address the spectrum properties that we investigated here.

This work aims at setting up a scheme which is able to efficiently predict the wavelength of absorption in the UV spectrum of chalcones, and using the scheme to examine the low-lying electronic transitions in chalcone, and assign the main transitions seen experimentally. To explore the effect of substitution on electronic spectra, we also investigate several derivatives with electron-donating substituent on phenyl ring.

2. Computational details

We have chosen the GAUSSIAN03 [18] program to perform geometry optimizations, vibrational frequency determinations

* Corresponding author. Tel.: +86 516 83262137.
E-mail address: xzmcysxue@sina.com (Y. Xue).

0166-1280/$ - see front matter © 2009 Elsevier B.V. All rights reserved.
doi:10.1016/j.theochem.2009.01.034

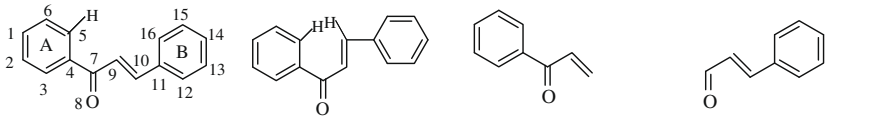

Scheme 1. Structures of the *s-cis* and *s-trans* conformers of *trans*-chalcone and its related compounds.

and excited state evaluations. The ground-state geometry of each molecule has been fully optimized with default thresholds on residual forces and displacements. Several schemes have been used for the optimization stage: Becker's three-parameter hybrid functional (B3LYP) [19,20], the one-parameter modified Perdew–Burke–Ernzerhof's functional (PBE1PBE) [21], the modified Perdew–Wang exchange and Perdew–Wang 91 correlation functional (mPW1PW91) [22], and BLYP [19,20]. In B3LYP, PBE1PBE and mPW1PW91, the percentage of exact, i.e., Hartree–Fock (HF), exchange amounts to 20%, 25% and 25%, respectively. It turned out that hybrid B3LYP, PBE1PBE and mPW1PW91 functionals combined with Pople's split valence double-ζ singly polarized atomic basis set, 6-31G(d), provides adequate results, especially for PBE1PBE and mPW1PW91 (see the following Section). For each geometry, vibrational frequencies were calculated analytically at the same level of theory as in the previous step, to ensure it to be a true local minimum.

After the ground-state geometry optimization, the excitation spectrum of each molecule has been computed with TD-DFT, using the 6-31G basis set and the PBE1PBE functional. During the TD-DFT calculations, the bulk solvent effects are considered by means of the polarizable continuum model (PCM) [23,24]. In PCM, one divides the problem into a solute part (chalcones) lying inside a cavity, and a solvent part (in this work, ethanol) represented as a structureless material, characterized by its dielectric constant as well as other macroscopic parameters. PCM is able to obtain a valid approximation of solvent effects as long as there is no specific interaction, such as hydrogen bonds, between the solute and the solvent. For this reason, aprotic solvents should be selected if experimental measurements have been performed in various media. In this study, however, we selected ethanol, with which the experimental measurements have been mainly performed. Moreover, properly taking into account such specific effects requires the determination of, at least, the first of the coordination spheres embedding each compounds. If this is technically possible for small systems [24], it would, nevertheless, require huge amounts of CPU time and would ruin our approach that we want as simple and as general as possible.

3. Methodological study

We have performed a methodological study on *trans*-(*s-cis*)-chalcone to assess the level of theory needed to obtain a reliable spectrum data. Tables 1 and 2 list the λ_{max} of chalcone calculated using several levels of theory.

We have started our investigations with the TD-B3LYP/6-31G(d)//B3LYP/6-31G(d) approach which has been found successful for propyl nitrate, indigoids and anthraquinone [26–28]. The methodological components of this strategy have been tested individually. In Table 1, we listed the excitation spectra obtained at the PCM-TD-B3LYP/6-31G(d) level based on the geometry optimized with various schemes, whereas in Table 2, the UV spectra were computed using different TD-DFT approaches for a given geometry.

From Table 1, one can see that convergence is reached when using the 6-311G(2d,2p) basis set. The extension of basis set from 6-31G to 6-311G(2d,2p) leads to a decrease in λ_{max}. The perfect agreement between 6-311G(2d,2p) and 6-311G(d,p) suggests that only one set of polarization functions is necessary. The agreement between 6-311G(d,p) and 6-31G(d) is also excellent. By comparing the excitation energies obtained with 6-31G(d) and 6-31+G(d), or 6-311G(d,p) and 6-311+G(d,p), it appears that including diffuse functions for the minimisation procedure has almost no effect on the λ_{max}. Therefore we have selected the 6-31G(d) for optimizing the geometry because it provides results close to 6-311G(2d,2p) with much lower computational costs. The differences between gas-phase and solvated geometries are small. For instance, at the B3LYP/6-31G(d) level, C4–C7, C7–O8, C7–C9, C9–C10 and C10–C11 distances are 1.503, 1.230, 1.484, 1.349 and 1.462 Å in the gas-phase and 1.500, 1.237, 1.479, 1.351 and 1.461 Å in ethanol, respectively. Consequently, the change in the UV spectra is limited to 2 nm when taking into account the solvent effects during the geometry determination process, probably due to the rigidity of the system. Obviously, the hybrid-DFT structures provide λ_{max} in better agreement with the experiment than pure-DFT (too large). The closest λ_{max} value is obtained with PBE1PBE and mPW1PW91. Therefore, we have selected the gas-phase PBE1PBE/6-31G(d) for determining the ground-state structural parameters.

Table 1
The λ_{max} (in nm) of *trans*-(*s-cis*)-chalcone obtained at the PCM-TD-B3LYP/6-31G(d) level on the geometries optimized with different schemes.[a]

Geometry	λ_{max}
B3LYP/6-31G	338
B3LYP/6-31G(d)	329
B3LYP/6-311G(d,p)	327
B3LYP/6-311G(2d,2p)	325
B3LYP/6-31+G(d)	330
B3LYP/6-311+G(d,p)	327
PCM-B3LYP/6-31G(d)	331
PBE1PBE/6-31G(d)	327
mPW1PW91/6-31G(d)	327
BLYP/6-31G(d)	338

[a] The experimental value (in ethanol) is 312 nm [25]/309 nm [11].

Table 2
The λ_{max} (in nm) of *trans*-(*s-cis*)-chalcone obtained with various TD-DFT schemes based on the geometries optimized at the PBE1PBE/6-31G(d) level.[a]

UV	λ_{max}
PCM-TD-PBE1PBE/6-31G	316
PCM-TD-PBE1PBE/6-31G(d)	318
PCM-TD-PBE1PBE/6-311G(d,p)	323
PCM-TD-PBE1PBE/6-311G(2d,2p)	324
PCM-TD-PBE1PBE/6-31+G(d)	329
PCM-TD-PBE1PBE/6-311+G(d,p)	331
TD-PBE1PBE/6-31G	299
PCM-TD-B3LYP/6-31G	325
PCM-TD-B3P86/6-31G	324
PCM-TD-B3PW91/6-31G	324
PCM-TD-mPW1PW91/6-31G	316
PCM-TD-PBE1PBE/6-31G	316
PCM-TD-B1LYP/6-31G	320
PCM-TD-BLYP/6-31G	363

[a] The experimental value (in ethanol) is 312 nm [25]/309 nm [11].

From Table 2, the 6-31G basis set gives the best result relative to experimental value. The energy difference between the 6-31G and 6-31G(d) basis being only 2 nm(0.03 eV) indicates that the addition of polarization functions does not bring any significant improvement to the calculation of excitation energies. Adding extra polarization function to 6-311G(d,p), increases the λ_{max} by only 1 nm, suggesting that the second set of polarization function is unnecessary. Adding diffuse function to 6-31G(d) or 6-311G(d,p) changes λ_{max} by +11 or +8 nm, respectively. Solvent effects tune the UV spectra (+17 nm) and should consequently be accounted for. We have used an extended panel of functionals for the TD-DFT calculations. The pure-DFT functionals provide too small excitation energies (+53 nm w.r.t. experiment for BLYP). All hybrid functionals are within 20 nm of the measured λ_{max}. By comparing the results of B3LYP, B3PW91, and B3P86, one sees that the correlation functional has no impact (less than 1 nm) on the excitation energies. This is well consistent with the results of previous investigations [29,30]. The best accuracy is reached by using the 25% functionals (B1LYP, mPW1PW91 and PBE1PBE), especially mPW1PW91 and PBE1PBE. The perfect agreement between them suggests that the form of the exchange functional does not matter, only the percentage of exact (HF) exchange included is crucial. For the sake of consistency, we have chosen PBE1PBE for TD-DFT calculation.

As the result of methodological consideration, the PCM-TD-PBE1PBE/6-31G//PBE1PBE/6-31G(d) approach has been selected for the study of the chalcones.

4. Results and discussions

4.1. Conformational analysis and molecular geometries

The α,β-double bond is always considered to exist in the *trans* configuration, since the *cis* configuration is unstable due to the strong steric effects between the B-ring and the carbonyl group. According to our calculation, the *trans* configuration is more stable than the *cis* one by 4.8 kcal/mol. IR studies [31,32] show two peaks for the C=O stretching mode which suggests that a second isomer, *trans*-(*s*-*trans*)-chalcone, coexists in solution with *trans*-(*s*-*cis*)-chalcone (see Scheme 1). The presence of this isomer could complicate the interpretation of the UV spectrum of *trans*-chalcone, as the two CO stretch peaks have intensity ratios of only 3:1–5:1. Thus, we performed the conformational analysis of both conformers. From the calculated equilibrium structure (see Fig. 1),we can see that the *s*-*cis* conformer seems to be fully planar, whereas steric hindrance between H atoms (see Scheme 1) leads the *s*-*trans* conformer to be nonplanar, with a torsion angle O8–C7–C9–C10 of approximately 5° and −152°, respectively. The difference in energy between the two conformers is 2.0 kcal/mol in favor of the *s*-*cis* compound, with a barrier of 6.6 kcal/mol from *s*-*cis* to *s*-*trans* form. Thus conversions between two conformers can take place easily, and *s*-*trans* conformer should exist in solution with *trans*-(*s*-*cis*)-chalcone under normal conditions. This is coinciding with the result of IR studies as mentioned above.

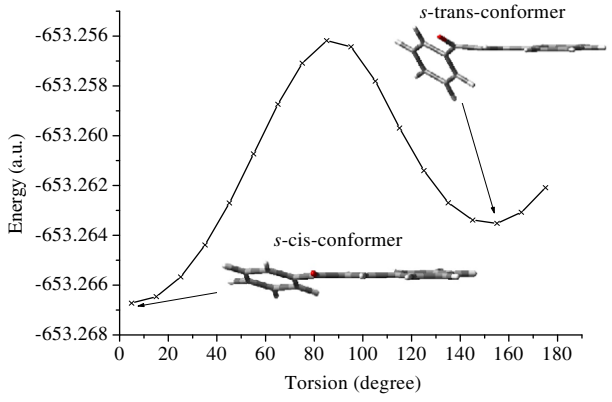

Fig. 1. Potential curve of the O8–C7–C9–C10 torsion angle in *trans*-chalcone.

Table 3
Selected key structural parameters of *trans*-chalcone from the DFT calculations and the X-ray experiments.[a]

Parameters	*s*-*cis*-conformer				*s*-*trans*-conformer
	B3LYP	PBE1PBE	mPW1PW91	Exp.[b]	PBE1PBE
Bond lengths (Å)					
R(4,7)	1.503	1.497	1.497	1.500	1.496
R(7,8)	1.230	1.225	1.224	1.205	1.224
R(7,9)	1.484	1.479	1.479	1.479	1.478
R(9,10)	1.349	1.345	1.345	1.320	1.346
R(10,11)	1.462	1.458	1.458	1.465	1.462
Bond angles (°)					
A(3,4,7)	117.5	117.4	117.4	117.6	117.6
A(4,7,8)	119.8	119.8	119.8	120.4	120.0
A(8,7,9)	121.1	121.2	121.2	121.1	119.0
A(7,9,10)	120.1	119.6	119.7	120.4	125.2
A(9,10,11)	128.1	128.0	128.0	127.6	127.1
A(10,11,12)	118.5	118.5	118.5	118.4	123.2

[a] Calculated values obtained with 6-31G(d) basis set.
[b] X-data from Ref. [33].

Table 3 lists the geometric parameters of *trans*-chalcone obtained at the B3LYP, PBE1PBE and mPW1PW91 theoretical levels with the 6-31G(d) basis set, as well as the X-ray data for the *s*-*cis*-conformer crystallized in ethanol [33]. It seems that the DFT-computed structural parameters of *s*-*cis* conformer are in well agreement with each other and with the experimental values. The deviations of the calculated bond lengths and angles are less than 0.03 Å and 1°, respectively, for all the three methods employed. Comparison of the calculated bond lengths and angles of the two conformers, we find that the corresponding values are not very much different, which indicate that conformational change has little effect on these geometrical parameters. The largest differences are less than 0.01 Å for bond lengths and 5.6° for angles.

4.2. Electronic spectra

All experimental data on the UV spectrum of *trans*-chalcone have been interpreted as the absorption of *trans*-(*s*-*cis*)-chalcone isomer, which is the main one we shall consider. To evaluate the influence of *s*-*trans*-conformer, the electronic spectrum of *trans*-(*s*-*trans*)-chalcone was also studied to clarify the spectral character further. Tables 4 and 5 presents the vertical excitation energies, the corresponding maximum absorption wavelengths, and oscillator strengths at the PCM-TD-PBE1PBE/6-31G//PBE1PBE/6-31G(d) level for *trans*-(*s*-*cis*)-chalcone and *trans*-(*s*-*trans*)-chalcone. For comparison, the CIS(D_1) theoretical values [15] and the experimental data for *trans*-(*s*-*cis*)-chalcone are also given. Tables 4 and 5 also give the weights of major configuration for each state.

It can be seen from Table 4 that the PBE1PBE excitation energies are in better agreement with experimental values than CIS(D_1), the deviations are usually only around 0.10 eV. The deviation for higher exited state 7 is slightly too large(~0.30 eV).

Comparing the results of *s*-*cis* and *s*-*trans* conformers (Tables 4 and 5), we can see that the two conformers present similar spectral properties. The *s*-*trans*-conformer also has five principal states corresponding to those of *s*-*cis*-conformer. The largest difference for excitation energies is only around 0.21 eV (16 nm). Moreover, the oscillator strengths and the transition character are also in good agreement with each other, respectively. Therefore, we could

Table 4
Calculated electronic transition (E, in eV) and oscillator strengths for *trans*-(*s-cis*)-chalcone in ethanol at PCM-TD-PBE1PBE/6-31G//PBE1PBE/6-31G(d) level.

States	Composition	This study			Exp.[a] $E(\varepsilon)$	CIS(D_1)[d] E (f)	Assign
		E	λ_{max}	f			
1	51 → 56 (38%) 54 → 56 (37%) 52 → 56 (15%)	3.5156	353	0.0008	3.50 (295)[b]	3.4948(<0.001)	Band I ($n \rightarrow \pi^*$)
2	55 → 56 (82%)	3.9273	316	0.9012	3.97[c]/4.01 (26700/23800)	4.8157(0.84)	Band II ($\pi \rightarrow \pi^*$)
3	52 → 56 (58%) 54 → 56 (33%)	4.4018	282	0.0215		5.0274(0.02)	
4	53 → 56 (90%) 55 → 59 (7%)	4.4127	281	0.0244		5.1018(0.08)	
5	51 → 56 (50%) 52 → 56 (18%) 54 → 56 (18%)	4.6604	266	0.0960	4.77 (6000)	5.5262(0.24)	Band III ($\pi \rightarrow \pi^*$)
6	55 → 57 (76%) 55 → 59 (8%)	5.5352	224	0.1078	5.39[c]/5.49 (8900/11200)		Band IV ($\pi \rightarrow \pi^*$)
7	53 → 57 (57%) 55 → 59 (26%)	6.4703	192	0.1950	6.17 (31526)		Band V ($\pi \rightarrow \pi^*$)

[a] Ref. [11], in ethanol.
[b] Ref. [11], in *n*-octane.
[c] Ref. [25].
[d] Ref. [15].

Table 5
Calculated electronic transition (E, in eV) and oscillator strengths for *trans*-(*s-trans*)-chalcone in ethanol at PCM-TD-PBE1PBE/6-31G//PBE1PBE/6-31G(d) level.

States	Composition	E	λ_{max}	f	Assign.
1	54 → 56 (51%)	3.6380	341	0.0048	$n \rightarrow \pi^*$
2	55 → 56 (75%)	4.1378	300	0.7394	$\pi \rightarrow \pi^*$
3	52 → 56 (80%)	4.5306	274	0.0078	
4	53 → 56 (88%)	4.5565	272	0.0158	
5	51 → 56 (52%)	4.7293	262	0.0899	$\pi \rightarrow \pi^*$
6	55 → 57 (72%)	5.4114	229	0.1095	$\pi \rightarrow \pi^*$
7	53 → 57 (54%)	6.3715	195	0.1807	$\pi \rightarrow \pi^*$

anticipate that the existence of *s-trans*-conformer in solution has little effects on the spectra of *s-cis*-conformer.

The spectrum of *trans*-(*s-cis*)-chalcone can be assigned with help of the calculated molecular orbitals, which are displayed in Fig. 2. It is a common feature of the lowest-energy transitions that they all involve the LUMO as the unoccupied orbital, the excitations to LUMO + 1 start at relatively high energies. The LUMO can be considered as the π^* orbital of the whole molecule.

The first excited singlet of chalcone is state 1 that can be assigned to the weak band at 3.50 eV (band I), which is a mixture of the HOMO-4 → LUMO (38%), HOMO-1 → LUMO (37%) and HOMO-3 → LUMO (15%) single electron promotions. Empirically this band would be described as a carbonyl $n \rightarrow \pi^*$ transition. In fact, by the calculations none of the occupied MOs can be visualized as a 'clean' *n*-orbital of the carbonyl group. In these MOs the n_{CO} orbitals are combined with the π orbitals of Ph_B and thus this transition has a mixed $n_{CO} \rightarrow \pi^*$ and $\pi_{PhB} \rightarrow \pi^*$ character. The extremely weak oscillator strength calculated for this transition is consistent with the fact that the corresponding experimental observed transition is a very weak shoulder to the red of the intense 4 eV absorption.

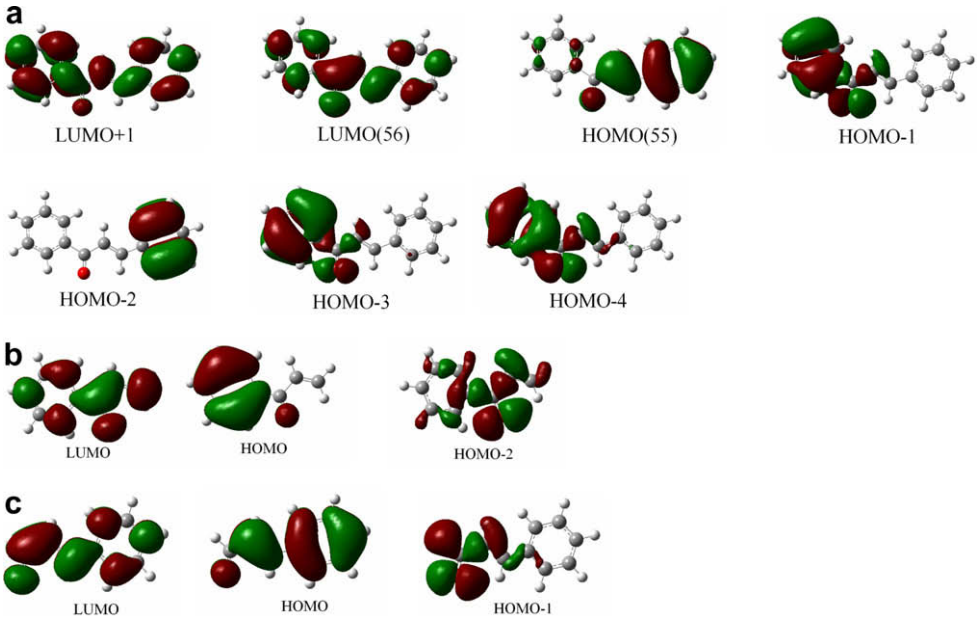

Fig. 2. Contour plots of the MOs for (a) *trans*-(*s-cis*)-chalcone, (b) *s-cis*-1-phenylpropenone and (c) *s-cis*-3-phenylpropenal.

The strong band at around 4 eV (band II) probably covers at least three electronic transition (states 2, 3 and 4). The 3rd and 4th transitions are nearly degenerated and have $\pi_{Ph} \rightarrow \pi^*$ character. For the 3rd transition the HOMO-3 → LUMO excitation is predominant, while in the other one the HOMO-2 → LUMO is predominant. The HOMO-2 and HOMO-3 are π orbitals of the two benzene rings, by shape they are the analogues of the HOMOs of toluene [34] and benzaldehyde [35], respectively. The peak at 4 eV with a very strong intensity is mainly composed of HOMO → LUMO configuration. From Fig. 2, HOMO is primarily localized on the 3-phenylpropenal and corresponds quite closely to the HOMO of *trans*-(*s-cis*)-3-phenylpropenal, which can be seen as a subsystem from substituting phenyl rings A in chalcone for hydrogen (see Scheme 1). Thus, this transition is of $\pi \rightarrow \pi^*$ character. We notice that our assignment of the very strong 4 eV absorption of *trans*-(*s-cis*)-chalcone to state 2 is different from the previous assertions, i.e., this peak is due to an electronic transition that is delocalized throughout the molecule [13,25,36]. Our assignment is generally consistent with the conclusions drawn from empirical PPP [11,37,14] and *ab initio* HF [15]calculations. It is worth noting that there is also a strong UV absorption of *trans*-(*s-cis*)-3-phenylpropenal at 4.3 eV [38,39], which mainly corresponds to the transition from HOMO → LUMO, and maps (with the same systematic 0.1 eV error) to our corresponding calculated excited states at 4.2 eV. This indirectly supports our assignment of band II.

The observed band III at around 260 nm can be seen as a shoulder to the blue of the strong peak due to band II. Our calculations suggest that state 5 corresponds to band III. This state is the combination of the one-electron excitation from the HOMO-4, HOMO-3 and HOMO-1, respectively, to the LUMO. From Fig. 2, this state is primarily localized on the 1-phenylpropenone part of the chalcone molecule and corresponds quite closely to the HOMO → LUMO ($\pi \rightarrow \pi^*$) excitation of *s-cis*-1-phenylpropenone. Thus, this transition has a mixed $\pi_{PhA} \rightarrow \pi^*$ and $\pi_{O8} \rightarrow \pi^*$ character.

We assign the states 6 and 7 to the bands IV and V, respectively. As shown in Table 4, state 6 is mainly due to the HOMO → LUMO + 1 one-electron excitation (76%), but configuration HOMO → LUMO + 3 is also involved. The state 7 consists of two principal configurations, i.e., HOMO-2 → LUMO + 1 and HOMO → LUMO + 3. These two states are all of $\pi \rightarrow \pi^*$ character.

4.3. Effect of substitution on band II

Given the localization of the intense electronic transition on the phenyl ring B, we anticipate that substitution with an electron-donating substituent will lower the excitation energy. By contrast, substitution on the phenyl ring A should only weakly affect the excitation energy. Thus, we have performed calculations on *trans*-chalcone derivatives which have a substituent in the para-position of the phenyl rings A and B, respectively. The calculated λ_{max} and shifts from *trans*-chalcone are shown in Table 6, together with the corresponding experimental results. It shows that the calculated λ_{max} are in good agreement with the experimental values, the absolute deviations range only from 0 to 12 nm, except for **d_2** and **e_2** (23 nm). In addition, the observed substituent effect is reproduced by calculation qualitatively. For instance, the ratio of calculated shift for **b_1** and **b_2** (~1:3) is in well agreement with the experimental value. This is also the case for others. By comparing, we find that the bathochromic effects of strongly positive electromeric substituents such as $N(CH_3)_2$, NH_2, OH, OCH_3, are 1.2–3.0 times greater when the groups are located on phenyl ring B than on ring A. Weakly positive groups such as CH_3 have small bathochromic effects when present on ring B and are practically no consequence when present on ring A. Thus, the λ_{max} of substituted chalcone in phenyl ring A is less sensitive to substitution than that in ring B. This is coinciding with the conclusion drawn in Section 4.2, i.e. the intense excitation corresponding to this peak mainly localized on the phenyl ring B.

Table 6
Calculated and observed *para*-substituent effects on the most intense electronic transition of *trans*-(*s-cis*)-chalcone (band II), at PCM-TD-PBE1PBE/6-31G//PBE1PBE/6-31G(d) level.[a]

Comp.	Substitution		λ_{max}		Shift	
	Ring A	Ring B	Calc.	Exp.[b]	Calc.	Exp.[b]
a_1	CH_3		317	308	1	−1
a_2		CH_3	326	330	10	21
b_1	CH_3O		326	320	10	11
b_2		CH_3O	343	341–345	27	32–36
c_1	OH		325	321, 325[c]	9	12, 13[c]
c_2		OH	343	351–355	27	42–46
d_1	NH_2		359	370	43	61
d_2		NH_2	377	400	61	91
e_1	$N(CH_3)_2$		386	393, 387[d]	70	84, 74[d]
e_2		$N(CH_3)_2$	402	425, 418[d]	86	116, 105[d]

[a] All experimental results in ethanol.
[b] Ref. [40,41], the shift is calculated on the basis of a 309 nm value for the parent compound.
[c] Ref. [42], the shift is calculated on the basis of a 312 nm value for the parent compound.
[d] Ref. [43], the shift is calculated on the basis of a 313 nm value for the parent compound.

From Table 6, it can also be found that the sequence of the λ_{max} are **a_1** < **b_1** ≈ **c_1** < **d_1** < **e_1** and **a_2** < **b_2** = **c_2** < **d_2** < **e_2** for substitution on phenyl ring A and B, respectively .These order are nearly identical to corresponding experimental results: **a_1** < **b_1** < **c_1** < **d_1** < **e_1** and **a_2** < **b_2** < **c_2** < **d_2** < **e_2**, respectively. The reason for the effect of substitution on absorption spectra is suggested that for the electron-donating substituents ($N(CH_3)_2$, NH_2, OH, OCH_3 or CH_3) on para-position, the lone electron pair of nitrogen or oxygen of $N(CH_3)_2$, NH_2, OH, OCH_3, and carbon–hydrogen σ-bond of CH_3 join in molecular conjugation, which makes the conjugated-system of molecules become larger. In addition, as the electron-donating ability of substituents is in the order of $N(CH_3)_2$ > NH_2 > OH > OCH_3 > CH_3, the sequence of the λ_{max} is **e** > **d** >**c** > **b** > **a**.

5. Conclusions

We have investigated *trans*-chalcone and its para-substituted derivatives using DFT and TD-DFT. Calculations permit assignments of the five lowest transitions seen experimentally. Our main conclusions are:

1. The PBE1PBE/6-31G(d) and PCM-TD-PBE1PBE/6-31G methods are successful for reproducing the molecular geometry and absorption wavelength, and suitable for studying chalcones. Conformational change has little effect on the bond lengths and angles and spectral properties.
2. The most intense electronic excitation in chalcone (band II) corresponds to a HOMO → LUMO ($\pi \rightarrow \pi^*$) transition that is largely localized within the 3-phenylpropenal part of the molecule.
3. Band I of chalcone is very weak and is an $n \rightarrow \pi^*$ transition. Band III, which is experimentally seen as a shoulder to the blue of band II appears to derive from state 5, which is quite closely related to a corresponding $\pi \rightarrow \pi^*$ excitation of *s-cis*-1-phenylpropenone. Bands IV and V mainly correspond to transitions from HOMO and HOMO-2, respectively, to LUMO + 1.
4. Observed substituent effect is reproduced by calculation qualitatively. The λ_{max} of substitution on phenyl ring A is less sensitive to substitution than that on ring B. The sequence of the calculated λ_{max} are nearly identical to corresponding experimental results.

Acknowledgement

This work was supported by the Science Research Startup Foundation of Xuzhou Medical College.

References

[1] S. Murakami, M. Muramatsu, H. Aihara, Biochem. Pharmacol. 42 (1991) 1447.
[2] R.J. Anto, K. Sukumarana, G. Kuttana, M.N.A. Raob, V. Subbarajuc, R. Kuttana, Cancer Lett. 97 (1995) 33.
[3] S. Ducki, R. Forrest, J.A. Hadfield, A. Kendall, N.J. Lawrence, A.T. McGown, D. Rennison, Biorg. Med. Chem. Lett. 8 (1998) 1051.
[4] F. Herencia, M.L. Ferrandiz, A. Ubeda, J.N. Dominguez, J.E. Charris, G.M. Lobo, M.J. Alcaraz, Bioorg. Med. Chem. Lett. 8 (1998) 1169.
[5] M. Liu, P. Wilairat, M.L. Go, J. Med. Chem. 44 (2001) 4443.
[6] S.N. López, M.V. Castelli, S.A. Zacchino, J.N. Dominguez, G. Lobo, J. Charris-Charris, J.C. Cortes, J.C. Ribas, C. Devia, A.M. Rodriguez, R.D. Enriz, Bioorg. Med. Chem. 9 (2001) 1999.
[7] J.H. Wu, X.H. Wang, Y.H. Yi, Bioorg. Med. Chem. Lett. 13 (2003) 1813.
[8] L. Mathiesen, K.E. Malterud, R.B. Sund, Planta Med. 61 (1995) 515.
[9] M.P. Cockerham, C.C. Frazier, S. Guha, E.A. Chauchard, Appl. Phys. B 53 (1991) 275.
[10] B. Zhao, D. Zhang, Y. Cao, W.J. Chen, Z.R. Sun, Z.G. Wang, Acta Phys. Chim. Sin. 16 (2000) 422.
[11] A.A. Sukhorukov, B.A. Zadorozhnyi, V.F. Lavrushin, Teor. Eksp. Khim. 6 (1970) 602.
[12] V.L. Gineitite, G.A. Gasperavichene, Teor. Eksp. Khim. 25 (1989) 271.
[13] K. Ohno, Y. Itoh, T. Harnada, M. Isogai, A. Kakuta, Mol. Cryst. Liq. Cryst. A 182 (1990) 17.
[14] K. Gustav, R. Colditz, A. Jabs, J. Prakt. Chem. 332 (1990) 645.
[15] M. Oumi, D. Maurice, M. Head-Gordon, Spectrochim. Acta 55A (1999) 525.
[16] L.D. Hicks, A.J. Fry, V.C. Kurzweil, Electrochim. Acta 50 (2004) 1039.
[17] D. Kozlowski, P. Trouillas, C. Calliste, P. Marsal, R. Lazzaroni, J.L. Duroux, J. Phys. Chem. A 111 (2007) 1138.
[18] M.J. Frisch et al., Gaussian 03, Revision B.03, Gaussian, Inc., Pittsburgh PA, 2003.
[19] A.D. Becke, J. Phys. Chem. 98 (1993) 5648.
[20] C. Lee, W. Yang, R.G. Parr, Phys. Rev. B 37 (1998) 785.
[21] J.P. Perdew, K. Burke, M. Ernzerhof, Phys. Rev. Lett. 78 (1997) 1396.
[22] C. Adamo, V. Barone, J. Chem. Phys. 108 (1998) 664.
[23] C. Amovilli, V. Barone, R. Cammi, E. Cancès, M. Cossi, B. Mennucci, C.S. Pomelli, J. Tomasi, Adv. Quantum Chem. 32 (1998) 227.
[24] M. Cossi, V. Barone, J. Chem. Phys. 115 (2001) 4708.
[25] H.H. Szmant, A.J. Basso, J. Am. Chem. Soc. 74 (1952) 4397.
[26] X.D. Gong, H.M. Xiao, J. Mol. Struct. (THEOCHEM) 498 (2000) 181.
[27] Y.S. Xue, X.D. Gong, H.M. Xiao, H. Tian, Acta Chim. Sin. 62 (2004) 963.
[28] Q.M. Zhang, X.D. Gong, H.M. Xiao, X.J. Xu, Acta Chim. Sin. 64 (2006) 381.
[29] V. Cavillot, B. Champagne, Chem. Phys. Lett. 354 (2002) 449.
[30] D. Jacquemin, J. Preat, M. Charlot, V. Wathelet, J.M. André, E.A. Perpète, J. Chem. Phys. 121 (2004) 1736.
[31] G. Venkateshwarlu, B. Subrahmanyam, Proc. Indian Acad. Sci. (Chem. Sci.) 102 (1990) 45.
[32] W.P. Hayes, C.J. Timmons, Spectrochim. Acta A 24 (1968) 323.
[33] D. Rabinovich, J. Chem. Soc. B (1970) 11.
[34] D.R. Borst, D.W. Pratt, J. Chem. Phys. 113 (2000) 3658.
[35] V. Molina, M. Merchán, J. Phys. Chem. A 105 (2001) 3745.
[36] O.H. Wheeler, P.H. Gore, M. Santiago, R. Baez, Can. J. Chem. 42 (1964) 2580.
[37] A.A. Sukhorukov, O.V. Lavrushina, V.H. Grif, V.P. Dzyuba, N.F. Pedchenko, B.A. Zadorozhny, B.F. Lavrushin, Zh. Obsch. Khim. (1978) 377.
[38] J.F. Thomas, G.E.K. Branch, J. Am. Chem. Soc. 75 (1953) 4793.
[39] L.A. Yanovskaya, G.V. Kryshtal, I.P. Yakovlev, V.F. Kucherov, B.Ya. Simkin, V.A. Bren, V.I. Minkin, O.A. Osipov, I.A. Tumakova, Tetrahedron 29 (1973) 2053.
[40] V. Alexa, Bull. Soc. Chim. Romania 18A (1936) 93.
[41] V. Alexa, Bull. Soc. Chim. Romania 1 (1939) 77.
[42] K. Shibata, T. Nagai, Chem. Soc. Japan 43 (1922) 101.
[43] E.R. Katzenellenbogen, G.E.K. Branch, J. Am. Chem. Soc. 69 (1947) 1615.